DOI 10.1007/s10593-023-03179-x
Chemistry of Heterocyclic Compounds **2023**, *59*(3), 171-178

A molecular electron density theory study of mechanism and selectivity of the intramolecular [3+2] cycloaddition reaction of a nitrone–vinylphosphonate adduct

Fouad Chafaa[1,2], Abdelmalek Khorief Nacereddine[2]*

[1] *Department of Basic Formation, Faculty of Natural and Life Sciences University of Batna 2, Batna, Algeria*

[2] *Laboratory of Physical Chemistry and Biology of Materials, Department of Physics and Chemistry, Higher Normal School of Technological Education-Skikda, Azzaba 21300, Skikda, Algeria; e-mail: a.khorief@enset-skikda.dz*

Published in Khimiya Geterotsiklicheskikh Soedinenii, 2023, *59*(3), 171–178

Submitted December 22, 2022
Accepted after revision January 27, 2023

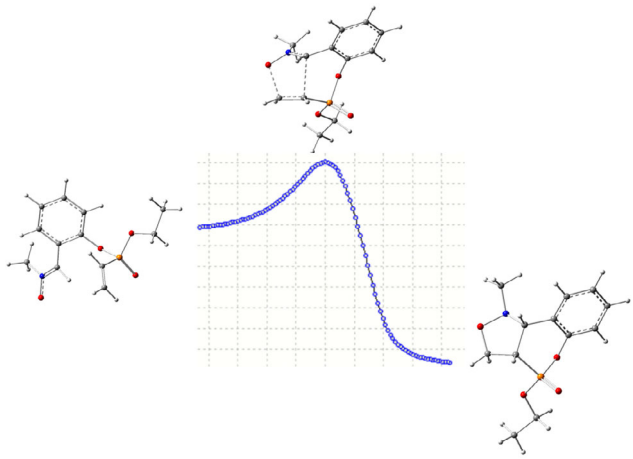

The selectivity and the molecular mechanism of the intramolecular [3+2] cycloaddition reaction of a nitrone–vinylphosphonate adduct was computationally studied within the molecular electron density theory using density functional theory method at the B3LYP/6-31G(d,p) level of theory. Conceptual density functional theory indices show that the nitrone–vinylphosphonate adduct has dual strong electrophilic and nucleophilic character. Local Parr functions reactivity indices reveal that this reaction favors the formation of the *fused* regioisomers in accordance with the experimental data. Analysis of different energetic profiles indicates that the *fused-endo* competitive pathway is favored kinetically, whereby this intramolecular reaction is characterized by exothermic and exergonic character. The geometry of transition states structures shows that the mechanism of this cycloaddition reaction is synchronous. Electron localization function topological analysis of the changes in electron density during the most favored reaction pathway shows that the mechanism is synchronous non-concerted.

Keywords: isoxazolidine, CDFT, cycloaddition, DFT, ELF, intramolecular reaction mechanism, MEDT, selectivity.

Heterocyclic compounds and their derivatives are of great interest in pharmaceutical research because they have diverse useful biological activities. Since many medicinal and pharmaceutical commercial substances contain a heterocyclic moiety in their structure, numerous experimental and theoretical studies have been performed to develop new economic and efficient synthetic methods for the preparation of these structures.[1]

One of the most exploited strategies for the preparation of various heterocycles, is the reactions of cycloaddition,[2] including the [3+2] cycloaddition (32CA) reaction.[3] The inter- and intramolecular 32CA reaction between nitrone (e.g., compound **1**) and ethylene (**2**) or its derivatives (alkenes) has found a wide use as an efficient method of synthesizing isoxazolidine heterocycles like compound **3** (Scheme 1).[3,4] Isoxazolidines have been used as starting

Scheme 1. 32CA reaction between nitrone **1** and ethylene (**2**) for the synthesis of isoxazolidine heterocycle **3**

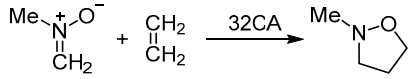

1 **2** **3**

materials or important intermediates for the synthesis of natural products and biologically active molecules.[5] These heterocycles have been shown to possess antimicrobial,[6] antifungal,[7] anti-inflammatory,[8] and antioxidant activity.[9]

Phosphonates are analogs of natural phosphates and phosphonic acid and are characterized by the presence of one or more C–P bonds. An interest related to these compounds has increased tremendously because of their potential as drugs (also prodrugs).[10] Phosphonates were observed to have antibacterial, anticancer, and antiparasitic activity.[10,11] These compounds can be also regarded as analogs of carboxylic acids, amino acids, and peptides.[12]

In recent years, the intramolecular 32CA reactions have been well studied experimentally and theoretically in order to understand the mechanism and the origin of the selectivity of this type of cycloaddition.[11,13–19] A major challenge in organic synthesis is to control the stereochemistry of the addition step. The stereochemistry of these reactions can be controlled either by choosing the appropriate reactants or by governing the reaction with a molecular complex acting as catalyst.[4] In some cases, cycloaddition reactions proceed through a stepwise mechanism.[17,20–24] Recent molecular electron density theory (MEDT)[25] studies of 32CA reactions involving the simplest three-atom components (TACs) have established a relationship between their electronic structure and reactivity.[26]

The intramolecular 32CA reactions of nitrones, leading to the formation of heterocycles *via* the *bridged* and/or the *fused* modes, constitute a versatile and efficient approach to the stereo- and regioselective construction of complex heterocyclic architectures having both nitrogen and oxygen atoms in a five-membered ring.[27,28] Recently Huang et al.[29] reported the intramolecular 32CA reaction of bifunctional nitrone–vinylphosphonate **6** prepared *in situ* from *O*-vinylphosphonylated salicylaldehyde **4** and *N*-methylhydroxylamine hydrochloride (**5**). The authors found that this 32CA reaction is characterized by complete *fused-endo* regio- and stereoselectivity in obtaining isoxazole derivative **7** (Scheme 2). The regioisomeric C3–C4 and O1–C5 reaction channel corresponds to the *fused* mode, while the C3–C5 and O1–C4 interaction corresponds to the *bridged* mode (Fig. 1).

Scheme 2. Synthesis of polycyclic phosphonated isoxazolidine **7** *via* an intramolecular 32CA reaction of nitrone–vinylphosphonate adduct **6**

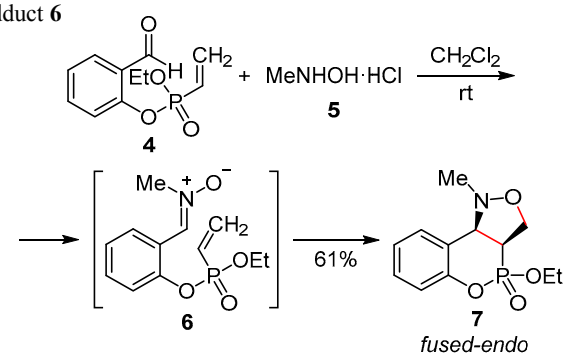

The main goal of this work is to undertake a theoretical study of intramolecular 32CA reaction of nitrone–alkene **6**, in which we investigate the experimentally observed selectivity, i.e., the regio- and stereoselectivity, in order to shed the light on the molecular mechanism of this reaction.

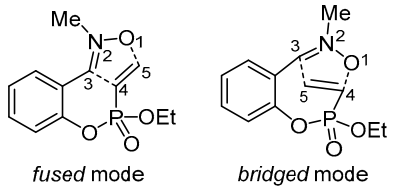

Figure 1. The *fused* and *bridged* regioisomeric modes of the intramolecular 32CA reaction of nitrone–vinylphosphonate adduct **6**, together with the numbering of the atoms involved in the reaction.

The present MEDT study has been divided into three parts; starting with the analysis of conceptual density functional theory (CDFT) reactivity indices, then energies and geometries, followed by the study of the nature of the molecular mechanism based on electron localization function (ELF) topological analysis. In the following investigation, the *E*-configuration of the nitrone double bond of adduct **6** will be used.

1. CDFT reactivity indices analysis

1.1. Global indices

The values of chemical potential (μ), chemical hardness (η), electrophilicity index (ω), and nucleophilicity index (*N*), as well as energies of frontier molecular orbital (FMO), i.e., the highest occupied molecular orbital (HOMO) and the lowest unoccupied molecular orbital (LUMO) of nitrone–vinylphosphonate **6** have been calculated as shown below (see Computation details) and collected in Table 1.

Table 1. Values of FMO energies and CDFT global reactivity indices (in eV) of nitrone–vinylphosphonate **6**

HOMO	LUMO	μ	η	ω	*N*
–5.51	–1.39	–3.45	4.12	1.44	3.61

From Table 1, we can notice that nitrone–vinylphosphonate **6** has a high electrophilicity index ω of 1.44 eV, being classified as the borderline between moderate and strong electrophile according to the electrophilicity scale.[30] On the other hand, compound **6** has also high nucleophilicity index and, therefore, may be classified as a strong nucleophile.[31] The polar 32CA reactions require participation of good electrophiles and good nucleophiles. Therefore, the intramolecular 32CA of nitrone–vinylphosphonate **6** will occur with a polar character demanding low activation energy.[32]

1.2. Local indices

In polar cycloaddition reactions involving the participation of non-symmetric reagents, the most favorable reaction channel is that involving the initial two-center interaction between the most electrophilic center of the electrophile and the most nucleophilic center of the nucleophile. In this context, Domingo et al.[33] proposed the electrophilic P_k^+ and nucleophilic P_k^- Parr functions, derived from the changes of spin electron density *via* the

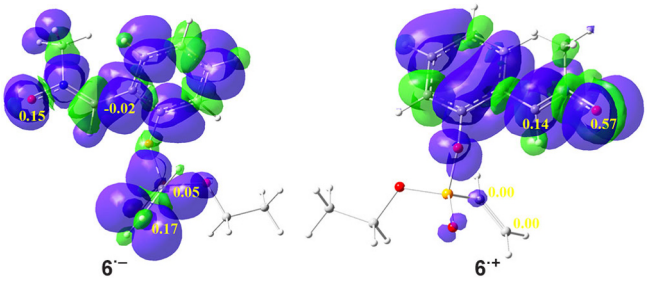

Figure 2. Maps of ASD representation of radical cation $\mathbf{6}^{\bullet+}$ and radical anion $\mathbf{6}^{\bullet-}$ of nitrone–vinylphosphonate **6** with local Parr function values on the reactive atoms.

global electron density transfer[34] process from the nucleophile to the electrophile, as powerful tools in the study of the local reactivity in polar processes. Accordingly, the electrophilic P_k^+ and the nucleophilic P_k^- Parr functions of nitrone–vinylphosphonate **6** were analyzed in order to characterize the most electrophilic and nucleophilic centers in this molecule involved in the intramolecular 32CA reaction and, thus, to explain the *fused* regioselectivity experimentally observed. The 3D representations of the atomic spin density (ASD) of the radical anion and the radical cation of nitrone–vinylphosphonate **6** including the values of electrophilic and nucleophilic Parr functions P_k^+ and P_k^- are given in Figure 2.

As shown in Figure 2, the electrophilic Parr functions P_k^+ of nitrone–vinylphosphonate **6** are mainly concentrated on the C4 carbon atom (P_k^+ 0.17) (see Figure 1 for atom numbering). On the other hand, the nucleophilic Parr functions P_k^- of nitrone–vinylphosphonate **6** are mainly concentrated on the O1 oxygen atom (P_k^- 0.57). Consequently, the most favored regioisomeric interaction will occur between the O1 oxygen atom and C4 carbon atom, giving the *fused* cycloadducts, as observed experimentally.[29]

2. Energies and geometries

The intramolecular reactions are characterized by a single reagent which reacts with itself to form a new product. Therefore, in the intramolecular 32CA reactions, the reagent contains two reactive parts, the TAC[35] part and the ethylene part. Thus, two reaction regioisomeric channels, namely the *fused* mode and the *bridged* mode, are possible in this intramolecular 32CA reaction. In addition, in each regioisomeric channel, there are two stereoisomeric approaches, the *endo* and *exo*. Thereby, in this intramolecular 32CA reaction, there are four possible transition states (TSs), *fused-endo* (**TSfn**), *fused-exo* (**TSfx**), *bridged-endo* (**TSbn**), and *bridged-exo* (**TSbx**), leading to the formation of four possible cycloadducts, **7fn**, **7fx**, **7bn**, and **7bx**, respectively (Scheme 3).

Table 2 shows the values of the relative electronic energies (in kcal·mol^{-1}) in gas phase and in solution of DCM, while total energies are given in Table S1 in Supplementary information file. These relative energies are calculated with respect to energy of nitrone–vinylphosphonate **6** that was taken as reference. From the analysis of the activation energies associated with the different reaction pathways we can notice that the *fused-endo* (**TSfn**) approach is the more kinetically favored (ΔE 8.41 kcal·mol^{-1}) one, the second favored approach is **TSbn** (ΔE 18.50 kcal·mol^{-1}, indicating for total regio- and stereoselectivity.

On the other hand, we can notice from the relative energies of the cycloadducts, that the *fused* and *bridged-endo* approaches are only under kinetic control, because of their exothermic character, while that of the *bridged-exo* (ΔE 38.08 kcal·mol^{-1}) is at the same time under kinetic and thermodynamic control due to its endothermic character. The instability of the *bridged-exo* cycloadduct **7bx** may be attributed to the high ring tension caused by the seven-membered ring. Therefore, the *fused* and *bridged-endo* pathways are irreversible processes and the *bridged-exo* pathway is reversible, and this intramolecular 32CA reaction thus leads to the formation of the kinetically favored cycloadduct **7fn** generated by the *fused-endo* pathway as a single regio- and stereoisomer, as observed

Table 2.The values of relative electronic energies, in gas phase and in DCM, of the TSs ($\Delta E^{\#}$, kcal·mol^{-1}) and cycloadducts **7** (ΔE, kcal·mol^{-1}) involved in the intramolecular 32CA reaction of nitrone–vinylphosphonate **6**

TS	$\Delta E^{\#}$		Product	ΔE	
	Gas phase	DCM		Gas phase	DCM
TSfn	8.41	10.60	**7fn**	–24.19	–21.59
TSfx	20.22	23.18	**7fx**	–21.33	–18.56
TSbn	18.50	18.89	**7bn**	–20.17	–18.57
TSbx	101.80	99.57	**7bx**	38.08	40.44

Scheme 3. The possible reaction pathways for the intramolecular 32CA reaction of nitrone–vinylphosphonate **6**

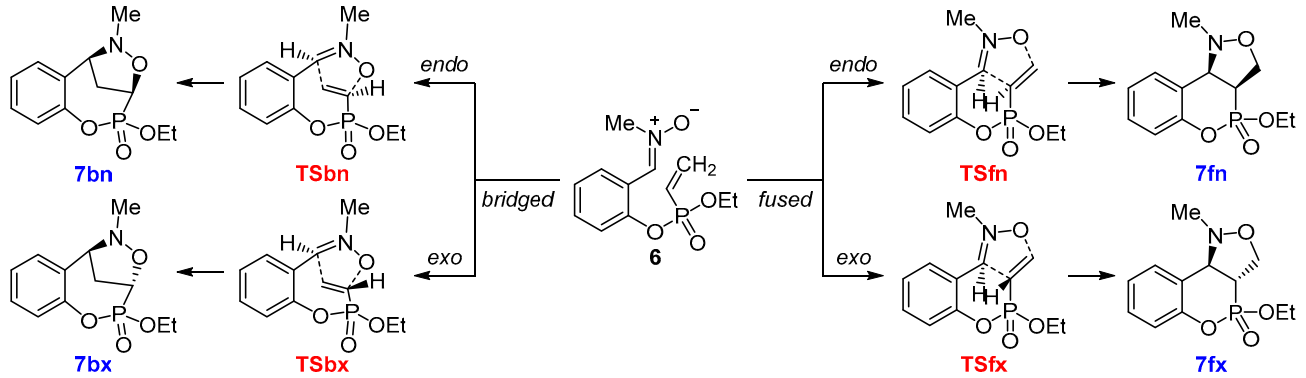

experimentally,[29] and in accordance with the local indices analysis based on Parr functions.

DCM was used experimentally as a reaction solvent, which can have a certain influence on the energy values in the case of the better solvation of the reagents. Table 2 clearly shows an increase in the activation energies of the *fused* modes in comparison with those obtained in the gas phase. These increases in *fused* mode energies are due to stabilization of the nitrone–vinylphosphonate **6** reagent in the DCM.[36] Note that for the non-favored *bridged* pathway (*bridged-exo*), we noticed a slight decrease of activation energy, but it is always the least favored pathway. The main change in activation energy is related to the more favored approach *fused-endo*, which amounts to 1.59 kcal·mol^{-1}. We can also observe that the solvent effects decrease the exothermic character of this intramolecular 32CA reaction by a values of 2.60, 2.77, 1.60, and 2.36 kcal·mol^{-1} for cyclization products **7fn**, **7fx**, **7bn**, and **7bx**, respectively. However, the solvent effects have no influence on the obtained gas phase regio- and stereoselectivities.

In order to take in consideration all the used experimental conditions, further calculations were performed which included the DCM solvent, temperature of 298K and 1 atmosphere of pressure. Thus, the values of relative enthalpies, entropies, and free energies for the intramolecular 32CA reaction of nitrone–vinylphosphonate **6** are collected in Table 3, while total energy values are given in Table S2 in Supplementary information file.

A comparison between the activation enthalpies indicates that the *fused-endo* mode (**TSfn**) leading to isoxazolidine **7fn** is still the most favorable approach by 4.75 kcal·mol^{-1} over the second most favored, i.e., *bridged-endo* mode (**TSbn**). In addition, the *fused* pathways and *bridged-endo* one are exothermic, while the *bridged-exo* is endothermic. Thus, the inclusion of thermal corrections in calculation does not change the selectivity and the thermal character obtained in the gas phase calculations.

On the other hand, we can notice that the values of relative activation entropies are low, which may be due to the unimolecular character of this 32CA reaction. The addition of entropic contribution to the enthalpies slightly increases the activation free energies by values in the range of 2–3 kcal·mol^{-1}, and always the *fused-endo* reaction pathway is the more favored one, **TSfn** having by about 4 kcal·mol^{-1} lower $\Delta G^{\neq}$ value than the second lowest value (*bridged-endo* path). Also, we can remark that the *fused* and the *bridged-endo* paths are exergonic, because they have negative relative free energies of the associated cycloadducts, while the *bridged-exo* path has an endergonic character, and therefore, it is the less favored path. Consequently, this intramolecular 32CA reaction of nitrone–vinylphosphonate **6** in DCM is characterized by an exothermic and exergonic characters favoring the formation of the *fused-endo* cycloadduct, in good agreement with experiment.

Table 3. Thermodynamic properties, namely, relative enthalpies ($\Delta H^{\#}$ and ΔH, kcal·mol^{-1}), relative entropies ($\Delta S^{\#}$ and ΔS, cal·mol^{-1}·K^{-1}), and relative free energies ($\Delta G^{\#}$ and ΔG, kcal·mol^{-1}), computed at 298K, 1 atm and in DCM solvent, of the TSs and cycloadducts **7** involved in the intramolecular 32CA reaction of nitrone–vinylphosphonate **6**

TS	$\Delta H^{\#}$	$\Delta S^{\#}$	$\Delta G^{\#}$	Product	ΔH	ΔS	ΔG
TSfn	13.95	–8.52	16.49	**7fn**	–19.50	–6.60	–17.53
TSfx	23.02	–7.59	25.28	**7fx**	–17.33	–14.71	–12.95
TSbn	18.70	–5.97	20.48	**7bn**	–16.84	–8.51	–14.31
TSbx	98.65	–4.18	99.90	**7bx**	41.53	–17.51	46.75

Figure 3 illustrates the optimized geometries of the TSs associated with the intramolecular 32CA reaction of nitrone–vinylphosphonate **6** together with the length of the new forming bonds. The Cartesian coordinates of the stationary points involved in the intramolecular 32CA reaction of nitrone–vinylphosphonate **6** together with the imaginary frequency of transition states are given in Supplementary information file.

From Figure 3, the lengths of the new O1–C5 and C3–C4 bonds in the *fused* mode are 1.921 and 2.321 Å for **TSfn** and 1.751 and 2.391 Å for **TSfx**, while for the *bridged* mode, the lengths of the newly formed bonds O1–C4 and C3–C5 are 2.199 and 2.077 Å for **TSbn** and 2.704 and 2.129 Å for **TSbx**. We clearly notice that the length of the C−O bond is shorter than that of the C–C bond, and if we take in consideration that a fully formed C–O bond is shorter than a C–C bond, we can conclude that the mechanism of formation of the new bonds is synchronous in the *fused* and *bridged-endo* pathways, and asynchronous in the unfavorable *bridged-exo* pathway.

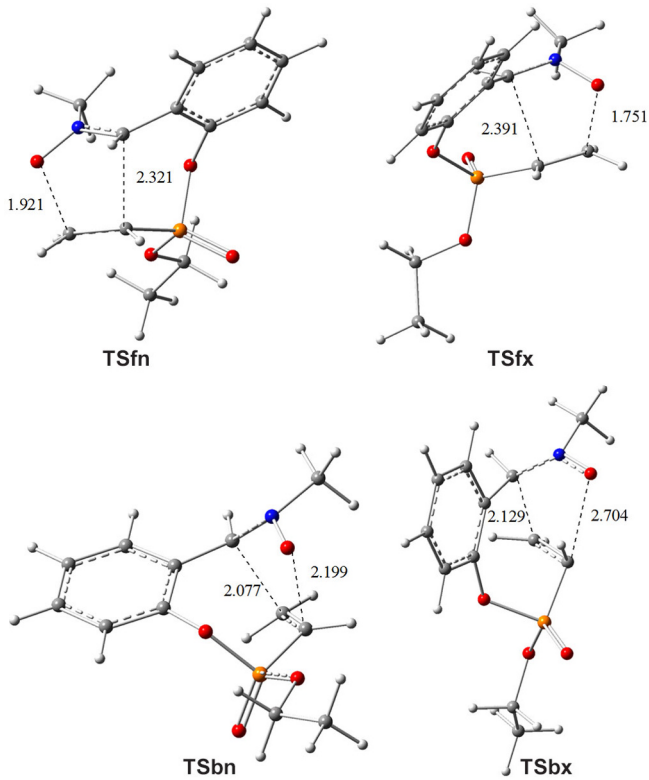

Figure 3. Optimized structures of the TSs associated with the intramolecular 32CA reaction of nitrone–vinylphosphonate **6** together with the lengths of the newly forming bonds (Å).

3. ELF topological analysis of the cleavage and formation of bonds

An attractive procedure that gives us a direct link between the distribution of electron density and the chemical structure is the quantum-chemical topological analysis of ELF established by Becke and Edgecombe.[37] In several studies we applied ELF topological analysis to different chemical systems in order to study the reaction mechanism and the reactivity of molecular systems.[21,23,38–40]

ELF localization domains and their attractor positions, together with the most representative valence basin populations of some pertinent points (**MC**, **TSfn**, **P1–3**, **7fn**) selected from the intrinsic reaction coordinate (IRC) curve (Fig. 4) are shown in Figure 5. ELF valence basin populations of these selected points corresponding to the formation of the O1–C5 and C3–C4 single bonds along the most favorable path (*fused-endo*) of the intramolecular 32CA reaction of nitrone–vinylphosphonate **6** are gathered in Table 4.

At the stage of molecular complex (**MC**), we can notice that the O1···N2···C3 and C4···C5 reactive regions of this system are characterized by two monosynaptic basins V(O1) and V'(O1) with a summary population of 5.90 e, accounting for the presence of three-electron non-pair region at the atomic center O1. The O1···N2 region is characterized by a valence basin with 1.34 e population associated to the O1−N2 single bond. In addition, we can notice the presence of V(C3,N2) disynaptic basin with population 3.99 e, which accounts for the C3=N2 double bond. On the other hand, the C4···C5 reactive region is characterized by the presence of two disynaptic basins V(C4,C5) and V'(C4,C5) with 1.70 and 2.09 e, respectively, accounting for C4=C5 double bond character.

At **TSfn**, the most noticeable change is the apparition of two V(C3) and V(C4) monosynaptic basins with 0.31 and 0.46 e of electron density, indicating the creation beginning of two reactive *pseudoradical* centers.[41] Also, a V(N2) monosynaptic basin appears at this point integrating 1.36 e which is associated with N2 non-bonding electron density region. This new electron population region is created from the decrease of electron density from the disynaptic basins V(C4,C5), V'(C4,C5), and V(C3,N2) that become populated 2.79 and 2.64 e, respectively. Note that the C4···C5 reactive region develops to contain only one disynaptic basin associated with the forming C4−C5 single bond.

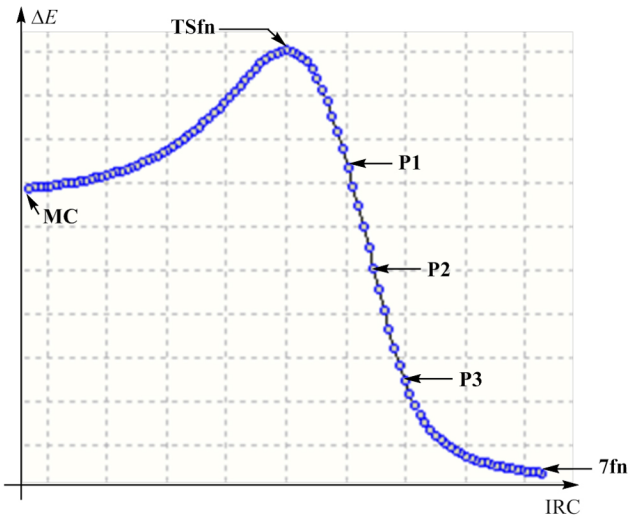

Figure 4. Relative energy curve of the *fused-endo* path of the intramolecular 32CA reaction of nitrone–vinylphosphonate **6** together with selected IRC points.

Table 4. ELF valence basin populations of the selected points at the IRC involved in the formation of the C3–C4 and O1–C5 single bonds along *fused-endo* path of the intramolecular 32CA reaction of nitrone–vinylphosphonate **6**. Electron populations are given in average number of electrons (e)

Valence basin	MC	TSfn	P1	P2	P3	7fn
V(C3,N2)	3.99	2.64	2.26	1.99	1.88	1.82
V(C4,C5)	1.70	2.79	2.25	2.01	1.94	1.89
V'(C4,C5)	2.09	–	–	–	–	–
V(O1)	3.02	2.96	3.34	2.64	2.60	2.57
V'(O1)	2.88	2.87	2.10	2.61	2.57	2.56
V(N2)	–	1.36	1.83	2.10	2.23	2.35
V(C3)	–	0.31	0.53	–	–	–
V(C4)	–	0.46	0.74	–	–	–
V(C3,C4)	–	–	–	1.55	1.71	1.82
V(O1,C5)	–	–	–	0.99	1.14	1.21

At the IRC point **P1**, which is the first selected point after **TSfn**, the main change is presented by the increase of electron density of the monosynaptic basins V(C3) and V(C4) to achieve 0.53 and 0.74 e, respectively. In the same time, the V(C4,C5) and V(C3,N2) disynaptic basins continue their depopulation to become 2.25 and 2.26 e, respectively.

At the IRC point **P2**, the remarkable change is the formation of two disynaptic basins V(O1,C5) and V(C3,C4) with a population of 0.99 and 1.55 e, respectively. These new basins are associated with the new forming C3–C4 and O1–C5 bonds. Thus, the formation of these disynaptic basins in the same point account for that the formation of the new bonds is slightly synchronous, in which the C3–C4 new bond is formed through *pseudodiradical* mechanism, while the O1–C5 one is formed *via* a dative mechanism through the donation of a part of the non-bonding electron density of the oxygen O1 atom to the C5 atomic center. In addition to the previous remarks, the electronic population of disynaptic basins V(C4,C5) and V(C3,N2) decreases slightly to 2.01 and 1.99 e, respectively.

At the IRC point **P3** which is the last point before the full formation of cycloadduct **7fn**, the electron density of the new V(O1,C5) and V(C3,C4) disynaptic basins increases to become 1.14 and 1.71 e, respectively. On the other hand, the electronic population of the V(C4,C5) and V(C3,N2) disynaptic basins slightly decreases further to arrive at 1.94 and 1.88 e, respectively.

Upon the arrival at cycloadduct **7fn**, which is the last point on the IRC curve, the population of the reactive basins changes slightly, whereby the values associated with

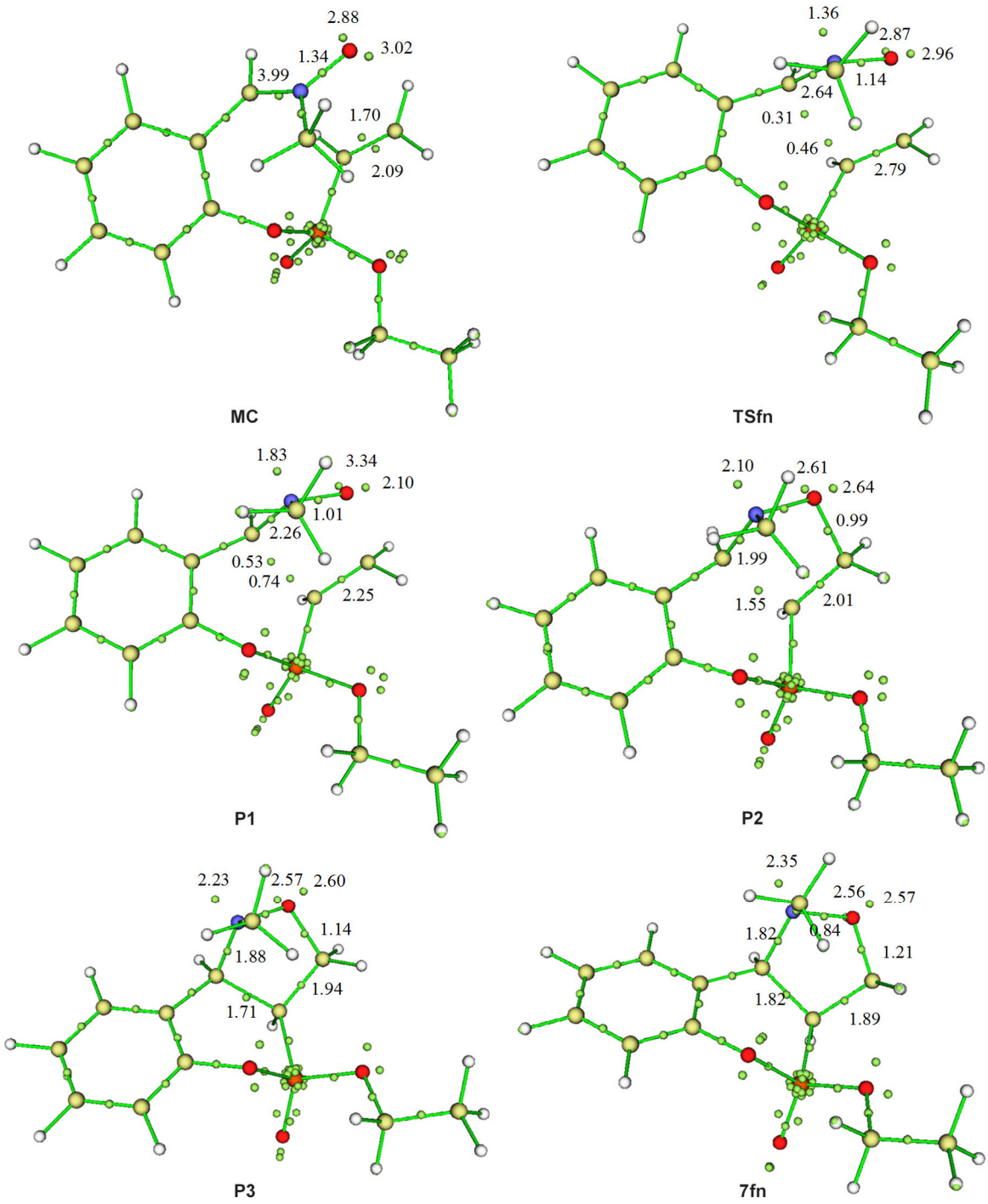

Figure 5. ELF basins attractor positions of relevant points of the IRC curve together with the populations of the relevant valence basins along the most favorable *fused-endo* path of the intramolecular 32CA reaction of nitrone–vinylphosphonate **6**.

the newly forming bond C3–C4 and O1–C5 increase to become 1.82 and 1.21 e, respectively, and those of the reactive region C3···N2 (V(C3,N2)) and C4···C5 (V(C4,C5)) decrease to 1.82 and 1.89 e, respectively.

In conclusion of this ELF topological analysis, the intramolecular 32CA reaction of the studied nitrone–vinylphosphonate adduct begins with decreasing bond order of the C4=C5 and C3=N2 double bonds forming *pseudo-diradical* centers at C3 and C4 atoms. These *pseudo-diradical* centers are necessary for the formation of the new C3–C4 bond. The second O1–C5 single bond is formed through the donation of part of the non-bonding electron density of the O1 oxygen on the C5 carbon. The two new bonds are formed simultaneously, which accounts for a synchronous non-concerted mechanism.

In this work, we have performed a MEDT study at the DFT B3LYP/6-31G(d,p) computational level of theory of the intramolecular 32CA reaction of a nitrone–vinylphosphonate adduct, in order to investigate the experimentally observed selectivity and to shed light on the

nature of molecular mechanism of this type of 32CA reaction. The main conclusions of this study are as follows:

1) CDFT reactivity indices analysis shows that the nitrone–vinylphosphonate adduct is a strong nucleophile and moderate electrophile which may undergo cyclization through a polar 32CA reaction with low activation energy.
2) Analysis of local reactivity indices based on Parr functions indicates that the main interaction is that between the most nucleophilic O1 atom center and the most electrophilic C5 atom center, leading to the formation of the *fused* regioisomers, as observed experimentally.
3) Analysis of energetic profiles, shows that the *fused-endo* reaction pathway is kinetically favored leading to the formation of the corresponding cycloadduct as a single product.
4) The presence of solvent DCM has no qualitative influence on the regio- and diastereoselectivity of the reaction, but it increases slightly the activation energies and decreases the exothermic character of this intramolecular 32CA reaction.
5) Analysis of thermodynamic parameters associated with this intramolecular 32CA reaction, indicates that it is exothermic and exergonic, characterized by low entropy values due to its monomolecular nature.
6) Analysis of TSs geometries indicates that this intramolecular 32CA reaction of the nitrone–vinylphosphonate adduct proceeds *via* a synchronous mechanism for the more favored pathways.
7) ELF topological analysis of the intramolecular 32CA reaction of cyclization shows that it proceeds through a non-concerted synchronous mechanism.

Computational details

In this theoretical study, for the geometry optimization of all stationary points, we have used the Gaussian 09 program.[42] The theoretical method used for this study is the DFT with the B3LYP hybrid functional in conjunction with the basis set 6-31G(d,p).[43,44] This level is shown to be suitable for geometry optimization and electronic property analysis of 32CA reactions and [4+2] Diels–Alder cycloaddition reactions.[23,38,40,45,46] The structures of the TSs have been confirmed by the existence of a single imaginary frequency and correspond to the new forming bonds. Several studies devoted to 32CA reactions have reported that the inclusion of solvent effects in the optimization of the geometry causes slight changes in the geometries of the gas phase.[13,47] Thus, the effects of DCM solvent were also taken into consideration through single point calculation from the gas phase optimized geometries using the polarizable continuum model[48] within the self-coherent reaction field.[49,50] Values of thermodynamic properties such as enthalpies, entropies, and Gibbs free energies in DCM were calculated using standard statistical thermodynamics at 298K and 1 atm through the optimized gas phase structures.[51] The natural bond orbitals method[52,53] was used for the analysis of electronic structures in TSs. The IRC[54] paths were traced in order to verify the energy profiles connecting each TS to the two associated minima of the proposed mechanism using the second order González–Schlegel integration method.[55]

The CDFT global reactivity descriptors,[56,57] i.e., the electronic potential (μ), the chemical hardness (η),[58] the electrophilicity index (ω),[59] and the empirical nucleophilicity index (*N*)[60] have been calculated from the energies of the FMO (HOMO and LUMO), according to the following equations: $\mu = (\varepsilon_{HOMO} + \varepsilon_{LUMO})/2$, $\eta = \varepsilon_{LUMO} - \varepsilon_{HOMO}$, $\omega = \mu^2/2\eta$, $N = \varepsilon_{HOMO(Nu)} - \varepsilon_{HOMO(TCE)}$, where, TCE is the abbreviation of tetracyanoethylene, which is taken as reference, because it has the lowest HOMO energy among most widely used ethylenic molecules.

The electrophilic (P_k^+) and nucleophilic (P_k^-) Parr functions[33] which enable characterization of the electrophilic and nucleophilic centers of a molecule were obtained by analysis of the Mulliken atomic spin density of the radical anion and the radical cation, respectively, of the studied molecule. Electronic structures of the selected structures were studied by ELF[37] over the B3LYP/6-31G(d,p) single determinant wave functions using the Multiwfn program.[61]

Supplementary information file containing values of total energies in gas phase and in dichloromethane, total enthalpies, entropies, and free energies, as well as the Cartesian coordinates of the stationary points involved in the intramolecular 32CA reaction of nitrone–vinylphosphonate **6** is available at the journal website http://link.springer.com/journal/10593.

This work was supported by the Ministry of Higher Education and Scientific Research of the Algerian Government (project PRFU Code: B00L01EN210120220001).

References

1. Kaur, N. *J. Heterocycl. Chem.* **2015**, *52*, 953.
2. Carruthers, W. *Cycloaddition Reactions in Organic Synthesis*; Pergamon Press: London, 1990. eBook; Elsevier, 2013.
3. Huisgen, R. In *1,3-Dipolar Cycloaddition Chemistry*; Padwa, A., Ed.; Wiley: New York, 1984, Vol. 1, p. 55.
4. Gothelf, K. V.; Jørgensen, K. A. *Chem. Rev.* **1998**, *98*, 863.
5. Berthet, M.; Cheviet, T.; Dujardin, G.; Parrot, I.; Martinez, J. *Chem. Rev.* **2016**, *116*, 15235.
6. Sadashiva, M. P.; Mallesha, H.; Murthy, K. K.; Rangappa, K. S. *Bioorg. Med. Chem. Lett.* **2005**, *15*, 1811.
7. Żelechowski, K.; Gołębiewski, W. M.; Krawczyk, M. *Monatsh. Chem.* **2015**, *146*, 1895.
8. Mullen, G. B.; Swift, P. A.; Georgiev, V. S. *J. Pharm. Sci.* **1987**, *76*, 930.
9. Kaur, M.; Singh, B.; Singh, B.; Arjuna, A. *J. Heterocycl. Chem.* **2017**, *54*, 1348.
10. Groaz, E.; De Jonghe, S. *Front. Chem.* **2020**, *8*, 616863.
11. Sennikova, V. V; Zalaltdinova, A. V; Sadykova, Y. M.; Khamatgalimov, A. R.; Gazizov, A. S.; Voloshina, A. D.; Lyubina, A. P.; Amerhanova, S. K.; Voronina, J. K.; Chugunova, E. A.; Appazov, N. O.; Burilov, A. R.; Pudovik, M. A. *Int. J. Mol. Sci.* **2022**, *23*, 14348.
12. Turhanen, P. A. *J. Biomed. Res. Environ. Sci.* **2022**, *3*, 195.
13. Duret, G.; Quinlan, R.; Yin, B.; Martin, R. E.; Bisseret, P.; Neuburger, M.; Gandon, V.; Blanchard, N. *J. Org. Chem.* **2017**, *82*, 1726.

14. Chafaa, F.; Hellel, D.; Khorief, A.; Djerourou, A. A. *Tetrahedron Lett.* **2016**, *57*, 67.
15. Chafaa, F.; Nacereddine, A. K.; Djerourou, A. *Lett. Org. Chem.* **2020**, *17*, 260.
16. Domingo, L. R.; Ríos-Gutiérrez, M.; Adjieufack, A. I.; Ndassa, I. M.; Nouhou, C. N.; Mbadcam, J. K. *ChemistrySelect* **2018**, *3*, 5412.
17. Jasiński, R.; Dresler, E. *Organics* **2020**, *1*, 49.
18. Jasiński, R. *Tetrahedron* **2013**, *69*, 927.
19. Sobhi, C.; Khorief Nacereddine, A.; Djerourou, A.; Ríos-Gutiérrez, M.; Domingo, L. R. *J. Phys. Org. Chem.* **2017**, *30*, e3637.
20. Żmigrodzka, M.; Sadowski, M.; Kras, J.; Dresler, E.; Demchuk, O. M.; Kula, K. *Sci. Rad.* **2022**, *1*, 26.
21. Barama, L.; Bayoud, B.; Chafaa, F.; Nacereddine, A. K.; Djerourou, A. *Struct. Chem.* **2018**, *29*, 1709.
22. Lamri, S.; Heddam, A.; Kara, M.; Yahia, W.; Khorief Nacereddine, A. *Organics* **2021**, *2*, 57.
23. Hamdaoui, H.; Khorief Nacereddine, A.; Djerourou, A. *J. Phys. Org. Chem.* **2022**, *36*, e4462.
24. Sadi, S.; Khorief Nacereddine, A.; Djerourou, A. *J. Phys. Org. Chem.* **2022**, *35*, e4311.
25. Domingo, L. R. *Molecules* **2016**, *21*, 1319.
26. Ríos-Gutiérrez, M.; Domingo, L. R. *Eur. J. Org. Chem.* **2019**, 267.
27. Koumbis, A. E.; Gallos, J. K. *Curr. Org. Chem.* **2003**, *7*, 585.
28. Tufariello, J. J. In *1,3-Dipolar Cycloaddition Chemistry*; Padwa, A., Ed.; Wiley: New York, 1984, vol. 2, p. 83.
29. Huang, T.; Wang, Q.; Kong, D.; Wu, M. *Tetrahedron Lett.* **2019**, *60*, 150913.
30. Domingo, L. R.; Aurell, M. J.; Pérez, P.; Contreras, R. *Tetrahedron* **2002**, *58*, 4417.
31. Jaramillo, P.; Domingo, L. R.; Chamorro, E.; Pérez, P. A *J. Mol. Struct.*: *THEOCHEM* **2008**, *865*, 68.
32. Domingo, L. R.; Sáez, J. A. *Org. Biomol. Chem.* **2009**, *7*, 3576.
33. Domingo, L. R.; Pérez, P.; Sáez, J. A. *RSC Adv.* **2013**, *3*, 1486.
34. Domingo, L. R. *RSC Adv.* **2014**, *4*, 32415.
35. Emamian, S.; Lu, T.; Domingo, L. R.; Heidarpoor Saremi, L.; Ríos-Gutiérrez, M. *Chem. Phys.* **2018**, *501*, 128.
36. Benchouk, W.; Mekelleche, S. M.; Silvi, B.; Aurell, M. J.; Domingo, L. R. *J. Phys. Org. Chem.* **2011**, *24*, 611.
37. Becke, A. D.; Edgecombe, K. E. *J. Chem. Phys.* **1990**, *92*, 5397.
38. Nacereddine, A. K. *J. Mol. Model.* **2020**, *26*, 328.
39. Yahia, W.; Nacereddine, A. K.; Djerourou, A. *Intl. J. Quantum Chem.* **2017**, *118*, e25540.
40. Chafaa, F.; Nacereddine, A. K.; Djerourou, A. *Theor. Chem. Acc.* **2019**, 123.
41. Domingo, L. R.; Sáez, J. A. *J. Org. Chem.* **2011**, *76*, 373.
42. Frisch, M. J.; Trucks, G. W.; Schlegel, H. B.; Scuseria, G. E.; Robb, Ma.; Cheeseman, J. R.; Scalmani, G.; Barone, V.; Mennucci, B.; Petersson, G. A.; Nakatsuji, H.; Li, X.; Caricato, M.; Marenich, A.; Bloino, J.; Janesko, B. G.; Gomperts, R.; Mennucci, B.; Hratchian, H. P.; Ortiz, J. V.; Izmaylov, A. F.; Sonnenberg, J. L.; Williams-Young, D.; Ding, F.; Lipparini, F.; Egidi, F.; Goings, J.; Peng, B.; Petrone, A.; Henderson, T.; Ranasinghe, D.; Zakrzewski, V. G.; Gao, J.; Rega, N.; Zheng, G.; Liang, W.; Hada, M.; Ehara, M.; Toyota, K.; Fukuda, R.; Hasegawa, J.; Ishida, M.; Nakajima, T.; Honda, Y.; Kitao, O.; Nakai, H.; Vreven, T.; Throssell, K.; Montgomery, J. A., Jr.; Peralta, J. E.; Ogliaro, F.; Bearpark, M.; Heyd, J. J.; Brothers, E.; Kudin, K. N.; Staroverov, V. N.; Keith, T.; Kobayashi, R.; Normand, J.; Raghavachari, K.; Rendell, A.; Burant, J. C.; Iyengar, S. S.; Tomasi, J.; Cossi, M.; Millam, J. M.; Klene, M.; Adamo, C.; Cammi, R.; Ochterski, J. W.; Martin, R. L.; Morokuma, K.; Farkas, O.; Foresman, J. B.; Fox, D. J. *Gaussian 09*, *Revision A.02*; Gaussian, Inc.: Wallingford, 2016.
43. Lee, C.; Yang, W.; Parr, R. G. *Phys. Rev. B*: *Condens. Matter Mater. Phys.* **1988**, *37*, 785.
44. Becke, A. D. *Phys. Rev. A*: *At., Mol., Opt. Phys.* **1988**, *38*, 3098.
45. Ríos-Gutiérrez, M.; Domingo, L. R.; Jasiński, R. *RSC Adv.* **2021**, *11*, 9698.
46. Mitka, K.; Fela, K.; Olszewska, A.; Jasiński, R. *Molecules* **2021**, *26*, 7147.
47. Layeb, H.; Nacereddine, A. K.; Djerourou, A.; Ríos-Gutiérrez, M.; Domingo, L. R. *J. Mol. Model.* **2015**, *21*, 104.
48. Tomasi, J.; Persico, M. *Chem. Rev.* **1994**, *94*, 2027.
49. Cancès, E.; Mennucci, B.; Tomasi, J. *J. Chem. Phys.* **1997**, *107*, 3032.
50. Cossi, M.; Barone, V.; Cammi, R.; Tomasi, J. *Chem. Phys. Lett.* **1996**, *255*, 327.
51. Becke, A. D. *J. Chem. Phys.* **1993**, *98*(7), 5648.
52. Reed, A. E.; Weinstock, R. B.; Weinhold, F. *J. Chem. Phys.* **1985**, *83*, 735.
53. Reed, A. E.; Curtiss, L. A.; Weinhold, F. *Chem. Rev.* **1988**, *88*, 899.
54. Fukui, K. *J. Phys. Chem*. **1970**, *74*, 4161.
55. Gonzalez, C.; Schlegel, H. B. *J. Chem. Phys.* **1991**, *95*, 5853.
56. Geerlings, P.; De Proft, F.; Langenaeker, W. *Chem. Rev.* **2003**, *103*, 1793.
57. Domingo, L. R.; Ríos-Gutiérrez, M.; Pérez, P. *Molecules* **2016**, *21*, 748.
58. Parr, R. G.; Pearson, R. G. *J. Am. Chem. Soc.* **1983**, *105*, 7512.
59. Parr, R. G.; Szentpály, L. v.; Liu, S. *J. Am. Chem. Soc.* **1999**, *12*, 1922.
60. Domingo, L. R.; Chamorro, E.; Pérez, P. *J. Org. Chem.* **2008**, *73*, 4615.
61. Lu, T.; Chen, F. *J. Comput. Chem.* **2012**, *33*, 580.